# Evolution in Structure and Morphology of Zirconium – Graphite Mixture under Mechanochemical Treatment in Hydrogen Flow

OL'GA S. MOROZOVA[1], CHRISTINA BORCHERS[2] and ALEXANDER V. LEONOV[3]

[1]*N. N. Semenov Institute of Chemical Physics, Ul. Kosygina 4, Moscow 117334 (Russia)*

*E-mail: om@polymer.chph.ras.ru*

[2]*Institute of Material Physic of the University of Goettingen, Hospital Str. 3–7, D-37073 Goettingen (Germany)*

[3]*M. V. Lomonosov Moscow State University, Chemical Department, Vorobyovy Gory, Moscow 119899 (Russia)*

## Abstract

Effect of mechanical activation on the structural transformations in zirconium – graphite – hydrogen system was studied using X-ray powder diffraction, scanning and transmission electron microscopy and kinetic techniques. Experiments with zirconium – graphite mixture were carried out under high-energy impact milling in a permanent hydrogen flow. Mechanically induced process of two stages was observed: (1) formation of the tetragonal e-$ZrH_x$ ($x$ = 1.8–2) phase, and (2) decomposition of the newly formed e-$ZrH_{1.8-2}$ phase into metal zirconium and zirconium hydride phases with lower hydrogen content. The transition from one stage to another is connected with the evolution in sample morphology. A loose and highly dispersed "composite" powder consisted of e-$ZrH_x$-containing fragments (2–30 nm in size) randomly distributed in the amorphous carbon, which were prepared at the first stage, transformed to larger compact particles with a fine multilayered structure at the second stage. Finally, the micron-size ribbon-like particles of partially crystallized graphite with Zr-containing fragments bimodal in size were formed. Carbon played a vital role in these transformations. No phases of zirconium carbide or zirconium carbohydride were detected in the reaction products.

## INTRODUCTION

The high-energy impact milling is a promising technique for synthesizing hydrides, nitrides, and carbides of IV b group metals from elements at room temperature [1–5]. Usually, these reactions are carried out at high temperature and pressure. Chemical transformations mechanically induced in binary systems (metal – hydrogen, metal – nitrogen, metal – carbon) are studied sufficiently in detail. The processes in ternary systems including metal, gas, and carbon are still only partially understood.

From the point of view of thermodynamics, formation of ZrC is preferable in a ternary system, as compared to that of $ZrH_2$ system due to the heats of ZrC and $ZrH_2$ formation ($\Delta H$ = −199.5 kJ/mol [6] и $\Delta H$ = −165 kJ/mol [7], respectively). From the point of view of kinetics, the formation of $ZrH_2$ in a ternary system is more preferable due to higher mobility of hydrogen. The aim of this work was to compare reactivity of carbon and hydrogen, when both react with zirconium. Chemical, phase, and morphological transformations in a zirconium – graphite – hydrogen system were studied with the use of X-ray powder diffraction (XRD), scanning (SEM) and transmission (TEM) electron microscopy, temperature-programmed reduction (TPR) and kinetic techniques.

## EXPERIMENTAL

Zirconium powder (purity of 99 %, $H_2$ content of 3–5 %) and graphite (chemically pure) were used as received. All the experiments were carried out at room temperature and atmospheric pressure in a hydrogen flow. The milling process was carried out under the following parameters: a vibration frequency of 50 Hz; an amplitude – of 7.25 mm; the average energy intensity was 1.0 kW/kg. A stainless steel flow mechanochemical reactor was loaded with 1.8 g of reaction mixture (1.5 g Zr + 0.3 g graphite) together with 19.8 g of hardened steel balls. The input of the reactor was connected to a setup for preparing gas mixtures; the outlet was combined on-line with a gas chromatograph to analyze the effluent gases. Hydrogen (99.5 %) was used as received. The duration of mechanical treatment was 15, 60, 85, 110, or 190 min. Specific surface area of powder ($S$) was measured by BET technique. XRD patterns of as-received and as-milled powders were recorded using a Dron-3 diffractometer with a Cu$K_a$ anode. The TPR was carried out at a heating rate of 12°/min from 20 to 550 °C under flow conditions (flow rate 100 ml/min.) using a $H_2$/Ar mixture with 7 vol. % of $H_2$. For SEM measurements, a Cameca MBX-1 microprobe in a regime of scanning microscopy was used. The TEM investigations were carried out on a Philips EM 420 ST electron microscope with a resolution limit of 0.3 nm and an accelerating potential of 120 kV. The TEM samples were prepared in an ethanol suspension and placed on copper grids covered by amorphous carbon.

## RESULTS AND DISCUSSION

Hydrogen consumption started immediately, as the mechanical activation started. The maximum sorption rate was observed in the first 10–20 min of milling (Fig. 1, curve *1*). The amount of hydrogen taken up was enough to form a stoichiometric zirconium hydride $ZrH_2$. In parallel, the $CH_4$ formation was detected from ~15 min to 90–100 min of treatment (see Fig. 1, curve *2*).

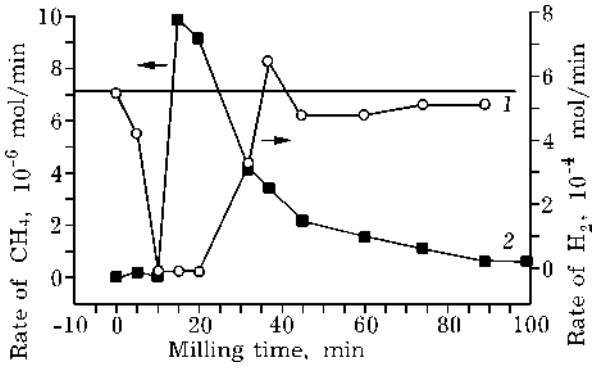


Fig. 1. Kinetic curves of hydrogen sorption (*1*) and $CH_4$ formation (*2*). $H_2$ flow rate: 5.6 $10^{-4}$ mol/min.

### *Phase transformation in the zirconium – graphite – hydrogen system*

Figure 2, a shows XRD patterns of original Zr (curve *1*) and powders tested after 15, 60, 85, 110, and 190 min of milling. The 15-min milled powder (curve *2*) consists of α-Zr, graphite, and zirconium hydride phase. The phase newly formed was identified as ε-$ZrH_x$, were $x$ = 1.8–2. According to TPR, ~80 at. % of Zr transformed to Zr-hydride during the first 15 min of milling, when the major hydrogen sorption occurs. Figure 2, *a* (curve *3*) shows that 60-min milled powder consists of graphite and ε-$ZrH_{1.8-2}$ phase. According to TPR, the sample still contains ~2 at. % of Zr. Figure 2, *a* (curve *4*) shows that only highly dispersed ε-$ZrH_{1.8-2}$ phase is present in the 85-min milled powder. TPR data confirm the absence of Zr in the sample. The XRD peaks of graphite disappear, which is indicative of amorphous graphite.The XRD pattern of 110-min milled powder (curve *5*) again contains α-Zr and graphite diffraction peaks, as well as a set of peaks assigned to γ-ZrH (JSPDS 2-862), δ-$ZrH_{1.66}$ (JSPDS 34-6490) and ε-$ZrH_{1.8-2}$ (Fig. 3).

The intensity ratio $I(002)/I(101)$ of the newly formed zirconium is significantly increased, as compared to that of original α-Zr. This indicates the plastic deformation of Zr microcrystals along the basal plain (0001). According to TPR, the sample contains ~20 at. % of Zr. Figure 2 (curve *6*) shows that the intensity of the diffraction peaks of δ-$ZrH_{1.66}$ and γ-ZrH phases markedly increase, while the peaks of ε-$ZrH_{1.8-2}$ phase nearly disappear after 190 min

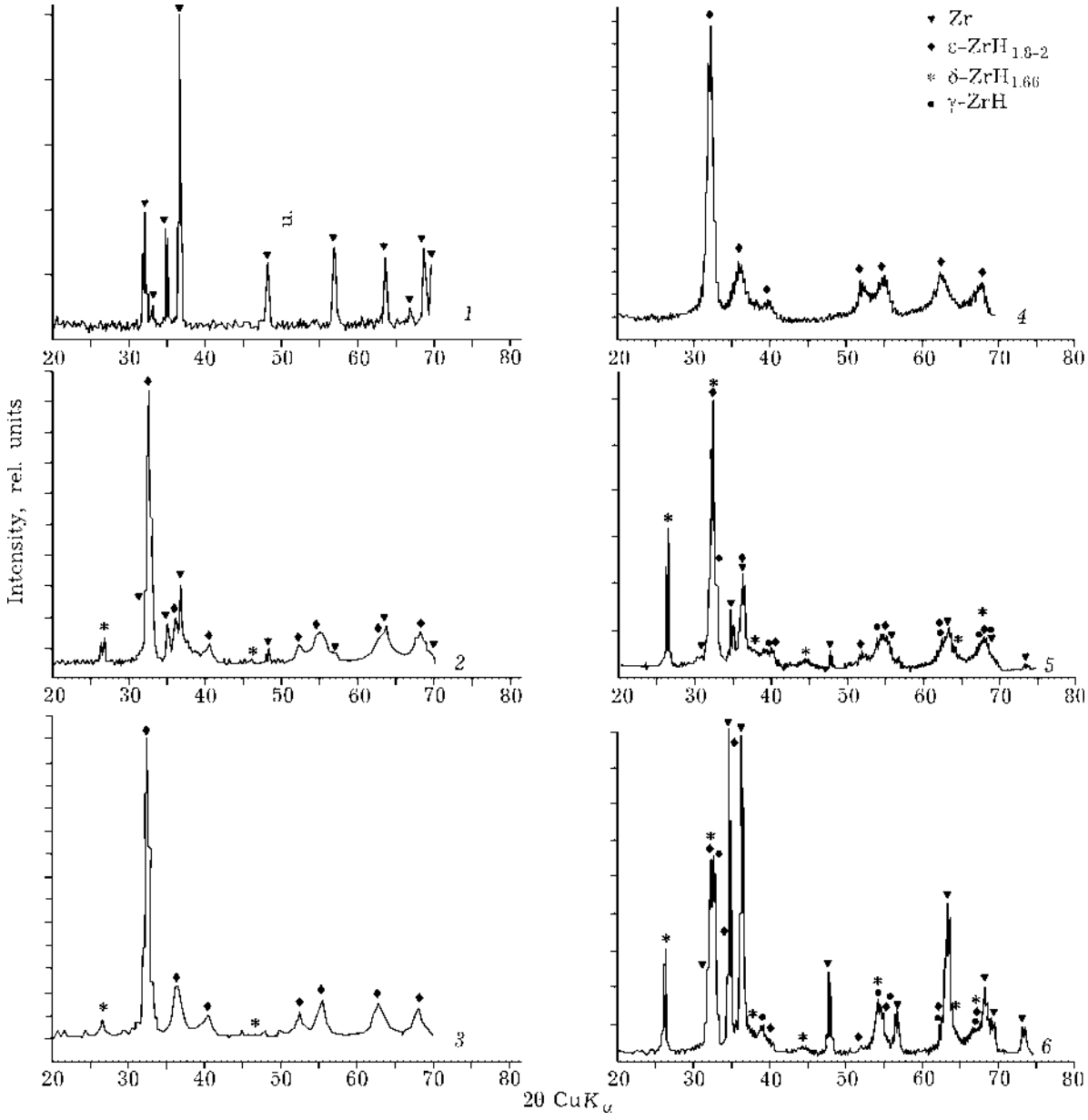


Fig. 2. XRD patterns: (*1*) initial Zr and Zr – graphite powders mechanically activated under $H_2$ flow for 15 min (*2*), 60 (*3*), 85 (*4*), 110 (*5*), and 190 min (*6*).

of milling. This suggests the decomposition of e-$ZrH_{1.8-2}$ phase. Intensities of a-Zr peaks also increase. Lattice constants of the newly formed a-Zr, are slightly enlarged ($a$ = 0.324 nm, $c$ = 0.515 nm), as compared to these of original a-Zr ($a$ = 0.323 nm, $c$ = 0.514 nm). The reason evidently is an insertion of C atoms into the metal lattice. According to TPR tests, the powder contains ~80 at. % of Zr.

No phases of zirconium carbide or zirconium carbohydride were detected in the mechanically activated zirconium – graphite powders.

Table 1 contains some characteristics of the samples on different steps of milling.

### *Morphological changes in the zirconium — graphite — hydrogen system*

Morphology of original Zr and Zr – graphite powders following different milling times is shown in Fig. 4. According to SEM, as-received Zr powder consists of "smooth surfaced" large particles on average size of ~50 mm (see Fig. 4, *a*). Mechanical treatment during 15–85 min fa-

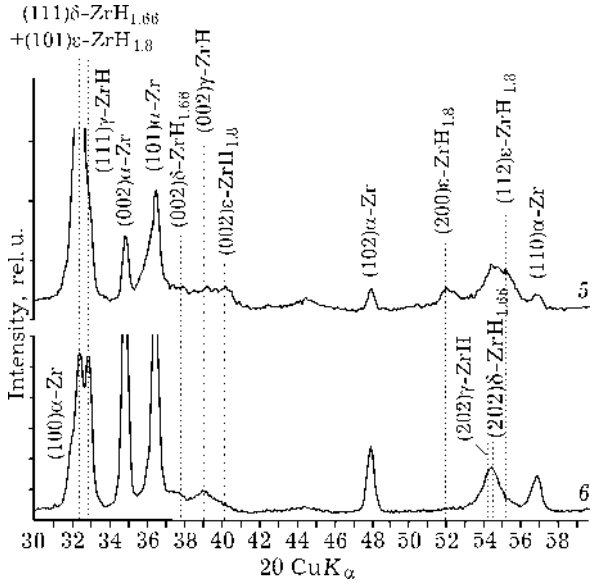


Fig. 3. Details of (*5*) and (*6*) patterns. See Fig. 2.

vours a decrease of average grain-size from 50 mm to 0.2–0.4 mm, which is in good agreement with an increase of the specific surface area from 0.6 to 58.4 $m^2/g$ (see Table 1 and Fig. 3, *b*, *c)*. Small particles are lumped together. After 110 min of milling, particles bimodal in size are observed. Surface of large particles is rough due to small particles placed on the external surface of larger ones. The large particles are of a flake-like morphology (see Fig. 4, *e*). Average particle size of 110-min and 190-min milled powders is ~25 and ~65 mm, respectively. This is in a good agreement with a drastic decrease in the powder specific surface area from 58.4 $m^2/g$ to 1.8 and 0.3 $m^2/g$, respectively (see Table 1 and Fig. 3, *c–e*). The 110-min milled powder contains particles larger than 150 mm and less than 0.2 mm, whereas the 190-min milled powder contains very few small particles.

According to TEM investigation, the 85-min milled powder consists of large loose aggregates (~200–250 nm) formed from small composite nanoparticles of more or less oblong shape about ~20–50 nm in projection. Each nanoparticle contains small ε-$ZrH_{1.8-2}$ "fragments" (2–30 nm in size) randomly distributed in amorphous carbon. After 110 min of milling, loose aggregates of small composite particles are transformed to compact particles of similar size with highly disordered microstructure. Thin layers (2–8 nm in width) of carbon and Zr-containing phases are intermixed. Separate fragments (less than 2–15 nm in size) of the randomly distributed Zr-containing phase also exist. Although such particles are quite typical for the powder tested, some others have macroscopic dimensions (several 100 nm). Large spherical carbon particles with spiral-like arranged layers are also observed.

190-min milling results in the further increase in the particle size and partial crystallization of Zr-containing fragments as well. Micron-size ribbon-like composite particles are formed. Carbon whiskers and nanotubes (20–80 nm in diameter) can be also seen on the

TABLE 1
Characteristics of initial and as-milled samples

| Characteristic | Initial reagent | | Mechanical activation time, min | | | | |
|---|---|---|---|---|---|---|---|
| | Zr | C | 15 | 60 | 85 | 110 | 190 |
| Phase composition | α-Zr | C | C, α-Zr, ε-$ZrH_{1.8-2}$ | C, ε-$ZrH_{1.8-2}$ | ε-$ZrH_{1.8-2}$ | C, α-Zr, γ-ZrH, δ-$ZrH_{1.66}$, ε-$ZrH_{1.8-2}$ (traces) | C, α-Zr, γ-ZrH, δ-$ZrH_{1.66}$, ε-$ZrH_{1.8-2}$ (traces) |
| Zr content, at. % (TPR) | | | ~20 | ~2 | 0 | ~20 | ~80 |
| $S$, $m^2/g$ | 0.34 | 2 | 8.7 | 25 | 58.4 | 1.85 | <0.3 |

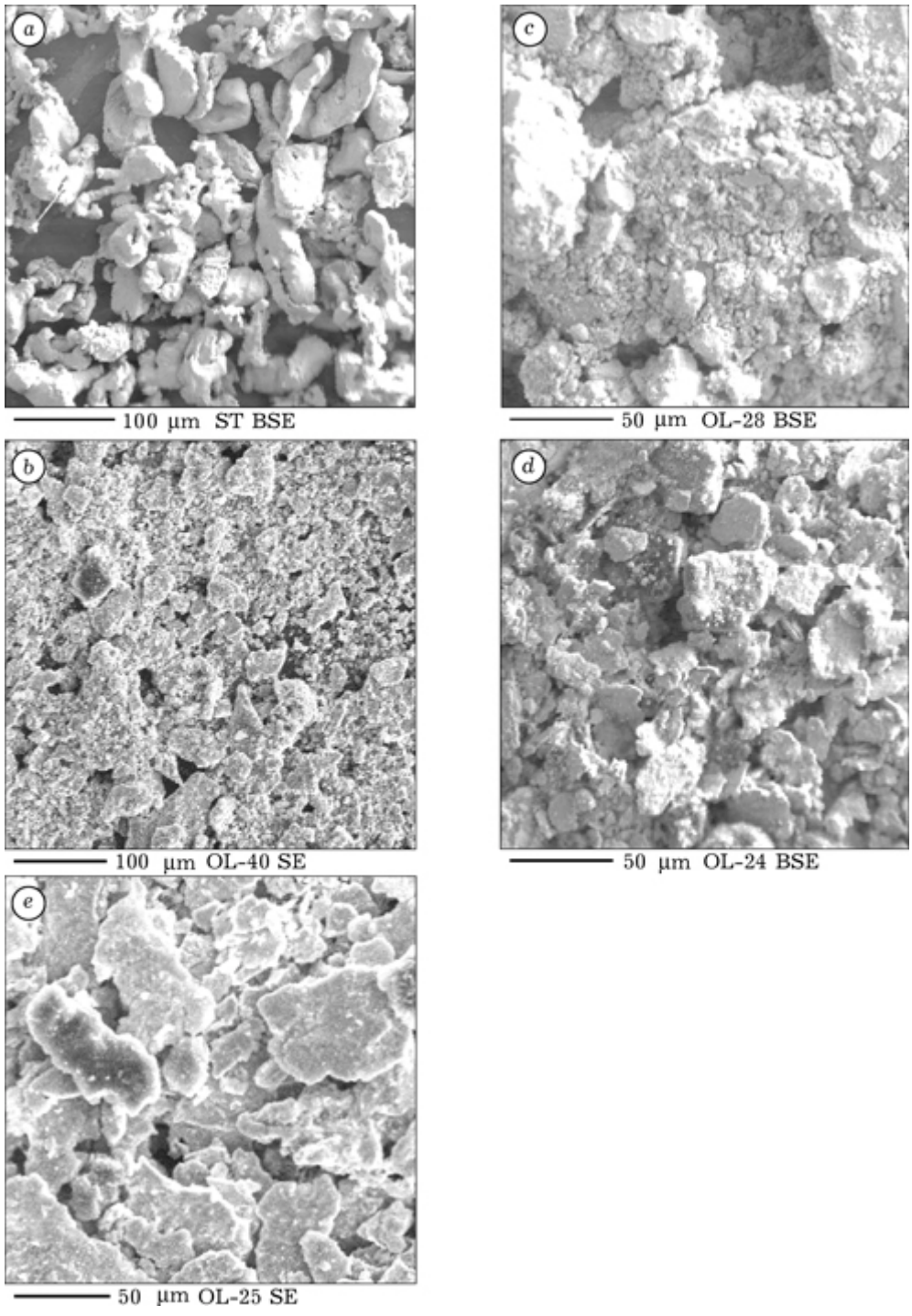


Fig. 4. SEM micrographs of initial Zr (*a*) and Zr – graphite powders after 15 min (*b*), 85 (*c*), 110 (*d*), and 190 min (*e*) of milling.

particle surface. The Zr-containing fragments from ~400 nm till several nm in size are randomly distributed in a carbon matrix.

As evident from the SEM and TEM data, the size of zirconium – graphite powder depends on milling time: it progressively decreases from several tens of micrometers to several nm and then increases again to several tens of micrometers. The "composite" material produced consists of Zr-containing fragments randomly distributed in a carbon matrix.

**DISCUSSION**

In context of chemistry of the studied process, it may be described as a two-stage process: (1) formation of the tetragonal ε-$ZrH_x$ ($x$ = 1.8–2) phase by the reaction

$$\alpha\text{-Zr} + H_2 \rightarrow \varepsilon\text{-}ZrH_{1.8-2}$$

and (2) decomposition of the newly formed ε-$ZrH_{1.8-2}$ phase by the reaction

$$\varepsilon\text{-}ZrH_{1.8-2} \rightarrow \delta\text{-}ZrH_{1.66} + \gamma\text{-ZrH} + \alpha\text{-Zr(C)} + H_2.$$

The ε-$ZrH_{1.8-2}$ phase is formed from the beginning of mechanochemical treatment due to the fast $H_2$ transportation to a juvenile zirconium surface. During the first 10–20 min of milling, the high rate of Zr – graphite powder disintegration is accompanied by the high rate of hydrogen sorption (see Fig. 1 and Table 1). This time is not sufficient for intermixing Zr and graphite on microscopic level, which is necessary for their interaction. At this stage, graphite being present in the reaction mixture stimulates the powder size reduction, as well as α-Zr conversion to ε-$ZrH_{1.8-2}$. In contrast to virtually constant specific surface area of Zr (0.4 $m^2/g$), the surface area of Zr – graphite powder was increased from 0.6 to 8.7 $m^2/g$ after 15 min of milling in $H_2$ flow. Conversion of to ε-$ZrH_{1.8-2}$ was 50 % for pure Zr, as compared to 80 % for Zr – graphite powder (see Table 1). After 85 min of treatment, the specific surface area of Zr – C powder was 58.4 $m^2/g$ due to brittle disintegration of Zr-hydride and effect of $H_2$ on the graphite specific surface area. The latter increases from 2 to 175 $m^2/g$ after 120 min of milling in $H_2$ flow. We suppose that the major part of the specific surface area of Zr – graphite powder comes from graphite. According to [8], graphite with large surface area has a large internal surface due to nanosized pores. Highly dispersed nanoporous graphite powder seems to make small Zr-containing fragments, which is distributed in graphite matrix, accessible for $H_2$ to produce ε-$ZrH_{1.8-2}$. Formation of $CH_4$ detected at this stage of treatment is the indirect evidence of this suggestion [9]. Zirconium was completely transformed to ε-$ZrH_{1.8-2}$ at the first stage of mechanical treatment.

The solid-state transformation ε-$ZrH_{1.8-2}$ → δ-$ZrH_{1.66}$ + γ-ZrH + α-Zr(C) + $H_2$ is the major reaction of the second stage. Decomposition of metal hydrides initiated by the mechanical treatment is well known [10, 11]. The special feature of the process studied is the decomposition of ε-$ZrH_{1.8-2}$ upon a permanent hydrogen flow, when ε-$ZrH_2$ with the highest hydrogen content (62.5 at. %) [12] is easily formed. According to Zr – H phase diagram, the transition ε-$ZrH_{1.8-2}$ → δ-$ZrH_2$ is a diffusionless transformation. It occurs when hydrogen content in ε-phase reduces from 62.5 to 61.4 at. % and hydrogen atoms remove from the tetrahedral sites in Zr-hydride lattice. The transition becomes more slow if contaminates, which occupy the octahedral sites [6, 12, 13], (oxygen, for example) are present. The broad two-phase ε + δ region is observed in this case. When hydrogen content falls to 60 at. %, the three-phase region (δ + metastable γ + α-Zr) is observed.

In our case, the hydrogen content in a ε-phase is stable until the surface of ε-$ZrH_{1.8-2}$ fragments is accessible for $H_2$. When these become blocked, the hydrogen content in ε-$ZrH_{1.8-2}$ falls down. The fact that the $CH_4$ formation stopped after ~100 min of milling is an indirect evidence of the surface blocked [9]. The progressive phase transition is indicative of impurities in a Zr-hydride lattice, namely, of carbon atoms, which occupy the octahedral sites, as well as oxygen atoms. The interstitial carbon atoms and structural defects seem to stabilize the metastable γ-ZrH phase and support the four-phase region (ε + δ + metastable γ + α-Zr), which is observed after 110 min of milling, but never was detected in the Zr – H phase diagram. The four-phase composition can be "frozen", if milling stopped. As milling starts again, the solid-state transformation goes further (compare Fig. 3, curves *5* and *6*).

The second stage of the process is induced by the drastic morphological changes: the loose particles of powder stick together to form the compact and large particles with a high concentration of strains. Specific surface area of the powder falls down from 58.4 $m^2/g$ to 1.8 and even to 0.3 $m^2/g$. Simultaneously, the intermixing of Zr-containing fragment with car-

bon on microscopic level is observed. The particles consist of thin carbon and Zr-containing nanolayers (2–8 nm in width) chaotically intermixed. These particles are believed to be something like a transition state of material. The interaction between carbon and $\varepsilon$-$ZrH_{1.8-2}$ is realized due to close contact of solid surfaces and significant extend of interfaces. As a result, carbon atoms incorporate through the surface into the Zr-hydride lattice to make the surface inaccessible for $H_2$. Carbon atoms being in the octahedral sites of $\varepsilon$-$ZrH_{1.8-2}$ lattice displace the H atoms from the nearby tetrahedral sites [13]. The decrease in hydrogen content initiates the $\varepsilon$-$ZrH_{1.8-2}$ decomposition. An increase in the $a$-Zr lattice constants indicates that carbon atoms are dissolved in the lattice of Zr, the product of $\varepsilon$-$ZrH_{1.8-2}$ decomposition.

The surprising thing is a sharp decrease in the specific surface area of reaction powder. According to [14], the graphite specific surface area initially increases and then 2–3 times decreases after about 3 h of milling in a stainless steel mill. More than 100-fold decrease, as compared to the maximum value, is observed in our case. The reason seems to be the modification of the powder surface by stable products of the partial graphite hydrogenation by active hydrogen of $\varepsilon$-$ZrH_{1.8-2}$ [9, 15]. These compounds are likely to change the mechanical properties of reaction powders through the powder surface modification. This phenomenon requires further investigation.

## CONCLUSIONS

Mechanical activation of the Zr – graphite mixture in a hydrogen flow was described as a two-stage process.

1. In a framework of the milling mechanism, the first stage is characterized by the formation of a highly dispersed composite material, whose loose particles contain nanofragments of Zr or $\varepsilon$-$ZrH_{1.8-2}$, embedded in an amorphous carbon matrix. In a framework of the chemical transformations, the first stage is characterized by a gas – solid reaction of $H_2$ with zirconium to form $\varepsilon$-$ZrH_{1.8-2}$.

2. In a framework of the milling mechanism, the second stage is characterized by sticking the loose particles in compact and large ones with a fine multi-layer structure. These particles evolve to ribbon-like particles including the Zr-containing fragments crystallized partially.

In a framework of the chemical transformations, the second stage is characterized by the decomposition of $\varepsilon$-$ZrH_{1.8-2}$.

Carbon plays a vital role in these transformations. However, no phases of zirconium carbide or zirconium carbohydride were detected in the reaction products.

## Acknowledgments

The authors are thankful to Prof. P. Yu. Butyagin, Dr. A. N. Streletsky (Institute of Chemical Physics, RAS), and Dr. A. Pundt (Institute of Material Physic of the University of Goettingen, Germany) for valuable comments and discussion, Dr. Khomenko (Institute of Chemical Physics, RAS) for performing TPR experiments, Dr H. Jander (Institute of Physical Chemistry of the University of Goettingen) for the preparation of TEM samples and N. Serebryakova (Institute of Physical Chemistry, RAS) for FTIR experiments. This work is supported in part by Ministry of Education, Science and Culture of Japan (grant (C) No. 12650692) and by Russian Foundation for Basic Research (project No. 01–03–32803).

## REFERENCES

1 A. Calka, J. I. Nikolov and B. W. Ninham, Proc. 2nd Int. Conf. on Structural Application of Mechanical Alloying, Vancowver, Canada, 1993, p.189.
2 A. Memezawa, K. Aoki and T. Masumoto, *Mat. Sci. Eng.*, A 181/ A 182 (1994) 1263.
3 A. Calka, *Appl. Phys. Lett.*, 89 (1991) 1568.
4 A. N. Streletskii, O. S. Morozova, I. V. Berestetskaya and A. B. Borunova, *Mater. Sci. Forum,* 269–272 (1998) 283.
5 A. N. Streletskii, O. S. Morozova, I. V. Berestetskaya *et al.*, *Ibid.*, 225–227 (1996) 539.
6 K. M. Maccay, Hydrogen Compounds of the Metallic Elements, E.& G. N. Spon LTD., London, 1966.
7 T. Ya. Kosolapova, Carbides, Metallurgiya, Moscow, 1968.
8 Y. Chen, J. Fitz Gerald, L.T. Chadderton and L. Chaffron, *J. Metastable and Nanocryst. Mat.*, 2–6 (1999) 375.
9 O. S. Morozova, A. V. Leonov, T. I. Khomenko and V. N. Korchak, *Ibid.*, 9 (2001) 415.

10 V. A. Teplov, V. P. Pilyugin, V. S. Gavikoet *et al.*, *Fizika metallov i metallovedeniye*, 84 (1997) 525.
11 A. N. Streletskii, O. S. Morozova, I. V. Berestetskaya *et al.*, *J. Metastable and Nanocryst. Mat.*, 8 (2000) 429.
12 R. L. Beck, *Transaction of the ASM*, 55 (1962) 52.
13 R. A. Andrievskii, Ya. S. Umanskii, Fazy vnedreniya, Nauka, Moscow, 1977.
14 H. Hermann, W. Gruner, N. Mattern *et al.*, *Mat. Sci. Forum*, 269–272 (1998) 193.
15 R. Q. Zhang, T. S. Chu, C. S. Lee and S. T. Lee, *J. Phys. Chem. B*, 104 (2000) 6761.